Structural effects on water adsorption on gold electrodes

Nuria Garcia-Araez[1,2], Paramaconi Rodriguez[2], Violeta Navarro[3], Huib J. Bakker[1], Marc T.M. Koper[2]

[1]FOM Institute for Atomic and Molecular Physics (AMOLF), Postbus 41883, 1009 DB Amsterdam, The Netherlands

[2]Leiden Institute of Chemistry, Leiden University, Postbus 9502, 2300 RA Leiden, The Netherlands

[3]Kamerlingh Onnes Laboratory, Leiden University, Postbus 9504, 2300 RA Leiden, The Netherlands

Abstract

We study the molecular properties of the interface formed between aqueous sulfuric acid solutions and gold electrodes by means of surface-enhanced infrared absorption spectroscopy (SEIRAS). The shape of the SEIRAS spectra is observed to be strongly dependent on the deposition rate with which the gold electrodes are prepared. We find that the water molecules coordinating to co-adsorbed sulfate anions become invisible in the SEIRAS spectra when the gold films are deposited at 1 Å/s, instead of the customary deposition rate of 0.1 Å/s employed in previous studies. AFM images of the gold deposits demonstrate that the increase of the gold deposition rate produces a decrease in the size of the nanoparticles composing the gold films. This suggests that water molecules co-adsorbed with sulfate anions on small gold nanoparticles are oriented parallel to the surface. On the other hand, the fact that these water molecules are not detected by SEIRAS facilitates the study of the adsorption of hydronium cations, since these SEIRAS bands overlap. It is concluded that the adsorption of sulfate anions does not involve the co-adsorption of any hydronium-water complex, since the SEIRAS band of the latter species exhibits a steady decrease with increasing potential.

1. Introduction

The interaction of water with metals plays a central role in many disciplines. In particular, the behavior of water at metal surfaces plays an important role in heterogeneous catalysis and electrocatalysis, and thus, a deeper understanding of the interaction between water and metals is crucial to improve the catalyst's function. An example of the importance of the role of water in electrochemical reactions is the dissociation of water at the electrified interface to form adsorbed OH or H that are key intermediates in oxidation or reduction reactions. Previous studies have shown that water has a promoting effect in the oxidation of CO and small alcohols on metal surfaces.[1,2] Water has also an important impact on the catalysis of the oxygen reduction reaction (ORR): water accelerates the oxidation of the metal in the presence of dissolved O_2, and this has a detrimental effect on the rate of the ORR, since the catalysis of the ORR only takes place on the metallic surface.[3-5]As a result, gold is potentially a better catalyst than platinum for the ORR, due to its higher oxidation potential. Indeed, deposition of gold nanoparticles on platinum has shown to improve the stability of the catalyst for the ORR.[6] However, the reduction of O_2 to H_2O on gold has only been reported in alkaline media on Au(100),[7,8] Au(100)-like polycrystalline gold,[9] and Au(100)-oriented gold nanoparticles,[10,11] and in sulfuric acid solutions on gold electrodes modified by gold nanoparticles.[12] Noteworthy, this latter study reported a marked effect of the size of the gold nanoparticles on the catalysis of the ORR. The authors attributed this effect to geometric changes of the gold surface (enriched concentration of step sites).

Unfortunately, the detailed molecular characteristics of surface water on metals have remained poorly understood, especially at electrochemical interfaces. This is because in most techniques the signal of surface water is overwhelmed by the response of the surrounding bulk water. In addition to this, the reactions that occur at the electrified solid-liquid interface are affected by the presence of ions and an external field. This fact increases the complexity to the reaction pathways and the elucidation of the reaction mechanism. One possible way to study water on metals is to decrease the amount of water on the metal to a few monolayers. This strict control of the system can be achieved under ultra-high vacuum (UHV) conditions,[13] but then, the experiments have to be performed at low temperatures and the electrochemical potential cannot be controlled. A successful strategy to study surface water on metals under electrochemical conditions is to measure FTIR spectra under conditions of attenuated total reflection (ATR). In this methodology, the electrode is a thin metal film deposited on a highly-refractive, transparent prism. The IR beam passes through the prism and is totally reflected at the metal-prism interface with an evanescent wave penetrating into the metal-solution interface, thereby probing the absorption of interfacial species. Under certain conditions, enhancement of the absorption signal of surface species takes place (SEIRAS: surface-enhanced infrared absorption spectroscopy). It has been shown that the enhanced electric field decays within a few monolayer distances from the surface.[14] As a consequence, the measured signal is dominated by the first few molecular layers of the electrolyte solution. Moreover, the contribution of the bulk background can easily be subtracted by calculating the difference of the measured spectra at different potentials. This methodology has been successfully applied to the study of interfacial water on gold thin films in previous studies.[15-35]

In this work we provide, for the first time, experimental evidence on the effect of the surface structure on the properties of water molecules adsorbed on gold electrodes. We show that that the SEIRAS bands of water co-adsorbed with sulfate anions vanish for gold films consisting of small grains. This is tentatively ascribed to the fact that, on small gold terraces, the adsorption of sulfate is more disordered, and co-adsorbed water molecules orient nearly parallel to the surface.

2. Experimental

The SEIRAS experiments were carried out with a Bruker Vertex80V vacuum FTIR spectrometer, equipped with a liquid-nitrogen cooled Hg-Cd-Te detector, employing the Kretschmann ATR configuration. The spectrometer operates at a pressure <1.8 hPa, so that interference due to the absorption of water vapors or CO_2 in the optical path is virtually eliminated. Leaking of the electrolyte solution towards the optical bench is avoided with the use of Teflon O-rings. The spectra were collected with p-polarized light with a resolution of 6 cm^{-1}. The incident angle was 60º from the surface normal. 16 interferograms were averaged for each spectrum, resulting in an acquisition time of 5 seconds per spectrum. During the experiments, the potential was scanned at 20 mV/s, and thus, each spectrum represents the average IR response of a potential interval of 100 mV. All spectra are presented as $\log(R_0/R_1)$, where R_1 and R_0 represent the intensities of the reflected beam at the sample and reference potentials, respectively. Positive adsorption bands correspond to species more strongly adsorbed at the sample potential, while negative adsorption bands are due to species more strongly adsorbed at the reference potential.

The gold thin layers were deposited on a silicon prism or on silicon wafers by using electron beam evaporation in a UHV system (pressure$<2x10^{-6}$ mbar). The evaporation rate and the final gold thickness were controlled with a quartz crystal microbalance. Prior to the experiments, the thin gold deposit was cleaned with acetone, isopropanol and thorough rinsing with ultra-pure water. The cell and all glassware were immersed overnight in a concentrated solution of $KMnO_4$ that was slightly acidic. Later the solution was removed and the residual MnO_2 was treated with a diluted solution of H_2O_2 and sulfuric acid (3:1) and finally thoroughly washed with ultra-pure water.

The electrochemical measurements were performed with an Autolab PGSTAT12. A gold wire was used as the counter electrode and a reversible hydrogen electrode (RHE) as the reference electrode. All potentials in this work are referred to the RHE scale. The electrical contact with the thin gold deposit was achieved with the help of a thin gold foil, which was not in contact with the solutions. Solutions were prepared from high purity reagents (H_2SO_4 from Aldrich triple distillated) and ultra-pure water (Millipore MilliQ gradient A10 system, 18.2 MΩ cm, <3 ppb total organic carbon). Ar (N66) was used to deoxygenate all solutions and CO (N47, stored in an aluminum cylinder and connected through aluminum valves, in order to prevent iron carbonyl contamination) was used to dose CO. For all the voltammograms presented here, the normalization of current to current density has been performed by using the geometrical area of the gold film in contact with the solutions (0.785 cm^2).

Ex-situ AFM images were acquired in air with a Nanoscope III (Digital Instruments) microscope in tapping mode using commercial cantilevers with silicon nitride pyramidal tips.

3. Results and discussion

Figure 1 shows the typical cyclic voltammograms of thin gold films with a thickness of 20 nm, deposited at 1 Å/s, and put in contact with an aqueous 0.1 M H_2SO_4 solution. No significant changes in the voltammograms were observed when the film thickness was varied between 20 and 30 nm, and when the deposition rate was varied between 0.1 and 1 Å/s.[36] The characteristic voltammetric profiles in figure 1 indicate that the gold films are clean and exhibit wide domains with (111) orientation. Three characteristic features evidenced the presence of Au(111) terraces: i) the pair of peaks at 0.6 V (P1), characteristic of the lifting of the reconstruction of Au(111) during the onset of sulfate adsorption,[37] ii) the pair of small, reversible peaks at 1.1 V (P2), associated to an order-disorder phase transition of adsorbed sulfate on Au(111),[37] and iii) the marked oxidation peak at 1.6 V(P3), characteristic of the surface oxidation of Au(111).[38] Previous SEIRAS studies reported similar voltammetric profiles of thin gold films deposited on silicon.[16,24]

Figures 2 and 3 show a series of typical SEIRAS spectra measured in a solution of 0.1 M H_2SO_4 with gold films prepared at two different deposition rates, namely, 0.1 and 1 Å/s, respectively. While the SEIRAS spectra in figure 2 are in good agreement with previous reports,[16,24] the results in figure 3, obtained with a faster deposition rate, appear markedly different. The differences in the SEIRAS spectra of figures 2 and 3 are not related to a difference in thickness of the gold layer. Essentially the same results are obtained with thickness varying between 20 and 30 nm.

All the spectra shown in Figures 2 and 3 are potential difference spectra with respect to a reference spectrum taken at E_{ref}=0.05 V. Therefore, positive bands correspond to species more strongly adsorbed at the sample potential, while negative bands are due to species more strongly adsorbed at the reference potential. At the reference potential employed here, E_{ref}=0.05 V, anion adsorption is negligible. For the assignment of the SEIRAS bands of the spectra in figure 2, we will mainly follow previous works:[16,24]

-The positive band at 1100-1200 cm^{-1}, whose magnitude markedly increases with increasing the applied potential, has been assigned to the S-O stretching mode, ν(SO), of adsorbed sulfate.

-Overlapping with the ν(SO) band, a small sharp negative band at 1115 cm^{-1} is observed, which is assigned to the Si-O stretching of silicon oxide, formed by oxidation of small patches of the silicon surface that are not covered by gold.

-For potentials E<0.7 V a negative band at 1615 cm^{-1} is observed that is assigned to the bending mode of adsorbed water, δ(HOH). At higher potentials, this band becomes a bipolar band, with a positive peak appearing at 1650 cm^{-1}, while the negative peak at 1615 cm^{-1} is still present.

-Upon close inspection, a small negative peak can be observed near 1700 cm^{-1}, which can be assigned to the bending mode of the adsorbed hydronium cation. In order to facilitate the observation of this band, the spectra in figure 2 have been enlarged within the bending mode region, the result of which is shown in figure 4A. This band is most visible at potentials between 0.4-0.8 V. The actual species corresponding to this band is probably not the H_3O^+ cation, but other hydronium-water complexes like $H_5O_2^+$, $H_7O_3^+$ and $H_9O_4^+$.[39]

-The negative band near 3470 cm^{-1} at E<0.5V can be assigned to the O-H stretch mode of adsorbed water, ν(OH). At potentials between 0.5 and 0.7 V, the ν(OH) band becomes bipolar, with a very broad positive peak near 3100 cm^{-1}. Then, at E≥0.8 V, the ν(OH) band becomes a positive band centered at 3490 cm^{-1}.

From the comparison of figures 2 and 3, it is concluded that:

-The ν(SO) band is little affected by the change in the gold deposition rate from 0.1 to 1 Å/s. Close inspection of figures 2 and 3 shows that the onset of the ν(SO) band is at 0.4 V with gold films made at 1 Å/s, while it is at 0.3 V with gold films deposited at 0.1 Å/s. However, the behavior of the ν(SO) band at higher potentials is very similar for both gold electrodes.

- For the gold films made at a faster deposition rate (1 Å/s), the δ(HOH) band appears as a single negative band centered at 1615 cm^{-1}, whose intensity increases with potential. The positive band at 1650 cm^{-1} is only observed for gold films deposited at 0.1 Å/s.

-Due to the absence of the positive δ(HOH) band at 1650 cm^{-1} for the gold films made at a faster deposition rate (1 Å/s), the negative band of the bending mode of the adsorbed hydronium cation near 1700 cm^{-1} is more clearly visible. For clarity, an enlargement of the spectra in the bending mode region is shown in figure 4B. It is observed that the central frequency of this negative band shifts from 1700 to 1670 cm^{-1} when the potential is increased.

- For the gold films made at a faster deposition rate (1 Å/s), the ν(OH) band appears as a single negative band whose central frequency slightly changes, from 3450 to 3500 cm^{-1} as the potential increases from 0.2 to 1.2 V. Overlapping with this band, at E>0.6V, a broad positive band centered near 3000 cm^{-1} is observed, which is also observed for lower gold deposition rates. However, the positive band centered at 3490 cm^{-1}, observed between 0.9-1.2V for gold films deposited at 0.1 Å/s, is fully absent.

At this point, it is useful to explain the potential dependence of the ν(OH) and δ(HOH) bands. At 0<E<0.5 V, it has been proposed that water is adsorbed with the hydrogen atoms somewhat closer to the metal, in such a way that the oxygen lone-pair orbital interacts with the gold surface (see figure 5A).[16,24] This orientation explains the relatively high frequency of the ν(OH) mode, 3450-3500 cm^{-1}, and the remarkably low frequency of the δ(HOH) mode, 1615 cm^{-1}. An additional negative δ(HOH) band is observed near 1700 cm^{-1}, which is due to hydronium-water complexes like $H_5O_2^+$, $H_7O_3^+$ and $H_9O_4^+$.[39] Indeed, the presence of $H_5O_2^+$ complexes on top of a water bilayer on Au(111) at E=0 V in 0.1M H_2SO_4 has been recently suggested based on distance tunneling spectroscopy.[40] At 0.5<E< 0.8 V, the appearance of the broad positive ν(OH) band near 3100-3000 cm^{-1} has been ascribed to water adsorption in an ice-like structure (see figure 5B).[16,24] DFT model calculations have shown that this is the most favorable structure of a water bilayer on Au(111).[41] At E>0.8 V, for gold deposits made at 0.1 Å/s, two new positive bands appear, namely, the ν(OH) and δ(HOH) bands centered at 3490 cm^{-1} and 1650 cm^{-1}, respectively. The magnitude of these bands markedly increases with potential, despite the fact that the coverage of adsorbed water species will probably decrease due to sulfate adsorption. These bands have been ascribed to water molecules coordinated with adsorbed sulfate, in particular, to water molecules bridging adjacent sulfate anions by hydrogen bonding to the oxygen atoms of sulfate (see figure 5C).[16] The coordination of water and sulfate in figure 5C follows the structures suggested from DFT calculations of sulfate on Pt(111)[42] and from distance tunneling spectroscopy on Au(111) in 0.1M H_2SO_4 at E=1.1 V.[43]

All species identified from the SEIRAS bands measured with gold films deposited at 0.1 Å/s seem to be also present with gold deposits at 1 Å/s, except for the sulfate-coordinated water molecules associated to the positive bands at 3490 cm^{-1} and 1650 cm^{-1}. This finding is surprising, especially taking into account that the ν(SO) band associated to adsorbed sulfate is little affected by the change in the gold deposition rate.

In order to assess if the marked differences in the SEIRAS spectra obtained at different gold deposition rates could be due to some difference in the topography of the gold films, we acquired ex-situ AFM images of the films. Representative images are shown in figure 6, for gold deposition rates of 0.1 and 1 Å/s. It is observed that, at both deposition rates, the gold films are formed by nanoparticles. The nanoparticle size clearly depends on the gold deposition rate: Gold films deposited at 0.1 Å/s are mainly composed of grains of 47±11 nm, while gold films made at 1 Å/s are mainly formed by grains of 27±8 nm (errors in grain size correspond to the standard deviation from the mean). The slower deposition rate allows a more dominant effect of the diffusion of atoms across the surface, leading to grain growth, grain coalescence and development of facets.[44,45] Similar results of the effect of the deposition rate on sputtered gold films on silicon have been reported previously.[46] Although the AFM images do not provide enough resolution to quantify the width of the Au(111) terraces, it can be expected that the change in the nanoparticle size will be accompanied by a similar change in the size of the Au(111) domains.

It should be recalled that sulfate adsorption on gold is very sensitive to the long range order of Au(111) terraces. High resolution STM images[37,47] have shown that sulfate adsorption on Au(111) leads to the formation of an extended superstructure with ($\sqrt{3}$ x $\sqrt{7}$) periodicity. High resolution STM images of Au(111) stepped surfaces[48] also demonstrated the presence of ($\sqrt{3}$ x $\sqrt{7}$) patches, even on rather narrow Au(111) terraces (12 atoms-wide terraces of 3 nm). However, the superstructure of adsorbed sulfate on Au(111) stepped surfaces showed the presence of several domains, separated by boundary areas with disordered structure. It was observed that, when the size of the Au(111) terraces is decreased, the size of the ordered ($\sqrt{3}$ x $\sqrt{7}$) domains also decreases, and the number of defects (domain boundaries, holes) within the adlayer increases. Therefore, it is concluded that sulfate adsorption on small Au(111) terraces will be more disordered.

Our SEIRAS measurements show that water molecules coordinating to co-adsorbed sulfate anions become effectively invisible in SEIRAS for gold films composed of small nanoparticles. This could be in principle ascribed to the fact that water molecules are completely removed from the interface by the adsorption of sulfate, but this explanation seems rather unlikely since sulfate anions bind strongly to water molecules.[49] Alternatively, it can be proposed that water molecules co-adsorbed with sulfate anions on small terraces are oriented nearly parallel to the surface. Consequently, these water molecules will not be detected in SEIRAS, since only vibrations that have dipole derivative components perpendicular to the surface are SEIRAS active.[50,51] DFT calculations of water monomers on Au(111) showed that the most stable orientation is nearly flat with respect to the surface.[41,52] Indeed, several SEIRAS studies have proposed that water adsorption on gold is nearly flat at potentials close to the potential of zero charge.[15,16,24,53] Here, we propose that water molecules will also lay flat when they are co-adsorbed with sulfate anions on small gold grains. Disordered adsorption of sulfate on small gold nanoparticles could result in a weaker interaction with co-adsorbed water molecules. Consequently, these water molecules will be rather isolated, mimicking the environment of the water monomers considered in the DFT calculations. It is also plausible that the effective charge density on the gold surface may be close to zero, as a result of charge-transfer from sulfate anions. Finally, it should be noted that, in some cases, granular films composed of small nanoparticles produce SEIRAS spectra with anomalous band shapes, such as bipolar or inverted bands. However, in the appendix we demonstrate that the gold thin films employed here produce SEIRAS spectra without distorted band shapes, since CO adsorption on these electrodes produces regular monopolar SEIRAS bands.

The present findings are not only useful to improve our fundamental understanding of the interface formed between gold electrodes and sulfuric acid solutions. They are also important to understand the catalytic performance. A previous study showed that the size of gold nanoparticles is a key parameter in determining the catalytic activity toward the reduction of oxygen.[12] Smaller gold nanoparticles decreased the overpotential for oxygen reduction, and produced the full reduction of oxygen to water. This behavior was tentatively ascribed to the different surface structure of the nanoparticles, such as the concentration of step sites. However, we have shown that the orientation of water molecules is also very sensitive to the size of the gold nanoparticles. Consequently, the full understanding of the improved catalysis of the oxygen reduction on small gold nanoparticles should also take into account the changes in the structure of the interfacial water network.

Finally, it is worth mentioning that it has been proposed that the adsorption of sulfate on gold involves the co-adsorption of H_3O^+ or $H_5O_2^+$ cations, instead of water molecules.[24,54] This point is related to some controversy on the interpretation of STM images. High resolution STM images of sulfate adsorbed on the (111) surfaces of Au, Rh, Pt, Pd and Ir identified the presence of weak tunneling spots in addition to the main bright spots in the ($\sqrt{3}$ x $\sqrt{7}$) unit cell.[37,47,54-59] In this superstructure, the total coverage of spots is 0.4 spots per gold surface atoms. By means of a careful thermodynamic analysis, Lipkowski and coworkers demonstrated that the saturation coverage of sulfate is 0.2.[60] Consequently, the bright spots in the STM images were ascribed to sulfate anions, while the weak spots were tentatively ascribed to co-adsorbed water molecules or hydronium cations.[16,24,54]

The present SEIRAS measurements obtained with gold films made at a faster deposition rate (1 Å/s, figure 3) allow the detailed study of the effect of potential on the band associated to hydronium-water complexes. These measurements do not suffer from the interference from the overlapping of the positive δ(HOH) band at 1650 cm^{-1} associated with water molecules coordinating to sulfate anions. It is observed that the intensity of the negative peak of the bending mode of the hydronium-water complexes, located near 1700 cm^{-1}, steadily increases with applied potential up to 1.2 V. This implies that the amount of hydronium-water complexes steadily decreases with potential. Hence, the present results strongly suggest that sulfate adsorption does not involve the co-adsorption of hydronium cations.

Noteworthy, the same conclusion was reached by Osawa and coworkers by means of SEIRAS measurements on gold thin films made at 0.1 Å /s.[16] They showed the data in a synchronous 2D spectrum, from which it was clear that sulfate adsorption does not lead to any cross peaks at the frequencies of hydronium bands. On the contrary, Wandlowski et al. showed the presence of a small SEIRAS band characteristic of hydronium-water complexes at potentials of sulfate adsorption.[24] Unfortunately, they presented the SEIRAS spectra using a reference spectrum taken at E=0.55V, and at this reference potential, a negative band due to hydronium-water complexes produced an artificial positive band in the spectra recorded at higher potentials. For this reason, they came to the erroneous conclusion that sulfate adsorption involves the co-adsorption of hydronium-water complexes. Indeed, in thermodynamic terms, the co-adsorption of sulfate anions and hydronium cations would be equivalent to the adsorption of bisulfate anions, and by means of a thermodynamic analysis, Lipkowski and coworkers demonstrated that the predominant adsorbed species on Au(111) in sulfuric acid solutions is sulfate, not bisulfate.[60]

4. Conclusions

We studied the properties of water at the interface between thin gold films and sulfuric acid solutions, as a function of the applied potential, using SEIRAS measurements. It is found that the rate at which the thin gold films were deposited on the silicon substrate has a major effect on the SEIRAS spectra of the interfacial water. While measurements performed with thin gold films deposited at 0.1 Å/s are in good agreement with previous works,[16,24] the results obtained with gold films made at 1 Å/s are strikingly different. Specifically, the SEIRAS bands assigned to water molecules coordinating sulfate anions are not present, whereas all other bands are identical to those observed on the films deposited at 0.1 Å/s. These results are explained with the help of ex-situ AFM images of the gold films. It is observed that gold films deposited at a higher rate are composed of smaller nanoparticles. A previous STM study of sulfate adsorption on Au(111) stepped surfaces showed that, on smaller Au(111) terraces, sulfate adsorption leads to the formation of a ($\sqrt{3}$ x $\sqrt{7}$) superstructure observed on extended Au(111) domains, but the number of defects (domain boundaries, holes) within the adlayer is significantly higher.[48] This indicates that sulfate adsorption on small gold nanoparticles is probably more disordered. Here, we tentatively propose that water molecules coordinating to sulfate anions on small gold nanoparticles lay flat with respect to the gold surface, thus explaining the fact that they are not detected in SEIRAS. This is supported by DFT calculations, which show that water monomers on Au(111) orient nearly parallel to the surface.[41,52] Finally, the present SEIRAS spectra provide a deeper understanding about the possibility of hydronium cation co-adsorption with sulfate anions. This possibility is ruled out in view of the fact that the SEIRAS band associated with the hydronium cations exhibits a steady decrease with increasing potential.

Acknowledgements

We gratefully acknowledge H. Zeijlemaker and H. Schoenmaker for their outstanding technical support, and T.H. Oosterkamp for providing generous access to the AFM facility. N.G.A. acknowledges the European Commission (FP7) for the award of a Marie Curie fellowship. M.K and P.R. acknowledge financial support from the Netherlands organization for Scientific Research (NWO) through a VICI and VENI grant.

Appendix: About anomalous band shapes in SEIRAS

Several works have reported SEIRAS spectra with anomalous band shapes, including asymmetrical and bipolar bands, and also bands with opposite sign than expected (the so-called inverted bands).[61-74] For this reason, the interpretation of SEIRAS bands has to be done with great care. Since SEIRAS bands with anomalous shapes are often observed on rough films consisting of small nanoparticles, one may argue that the spectra measured with films composed by small grains (figure 3) are distorted. However, below we demonstrate that this is not the case.

Several theories have been developed to explain the observed SEIRAS anomalous band shapes. 1) Fano[75] proposed that this behavior originates from the nonadiabatic interaction of adsorbed species with a continuum of electronic excitations. This effect is called the Fano resonance effect, and the corresponding mathematical expressions have been derived by Langreth.[76] 2) Alternatively, Persson and Volokitin[77] proposed that the nonadiabatic interaction is due to the coupling of the adsorbate vibrations to the excited electron motion via surface-friction terms. 3) On the other hand, Osawa[14] explained the anomalous band shapes through the calculation of the electromagnetic enhancement within the effective medium theory. In this framework, SEIRAS spectra are calculated by using Fresnel equations and an appropriate expression for the effective dielectric function of the sample, the latter being estimated by the Maxwell-Garnet and the Bruggenman methods. Quantitative agreement between the experiments and the calculations, even with bipolar bands and inverted bands, was accomplished.[61] 4) Following a similar method to Osawa's, Griffiths et al.[62] also used effective medium theory to explain quantitatively anomalous band shapes in SEIRAS. However, they used the Bergman representation of the effective dielectric function, and with this, they concluded that anomalous band shapes appear with thin metal film near percolation. 5) Finally, Bürgi[65] demonstrated that the appearance of anomalous band shapes is also predicted by classical electromagnetic theory, under certain conditions, even when the dielectric function of the metal equals to that in the bulk.

Noteworthy, experiments show that the appearance of anomalous bands is correlated to the specific properties of the underlying thin metal film (most importantly, the film morphology, which is closely related to the method of preparation).[61-64,66-72,74] All the above cited theories agree on that point. Therefore, although it is difficult to predict if a particular method of preparation of thin metal films will produce anomalous SEIRAS spectra, it is possible to test the properties of the metal film with a test molecule, and then conclude if the spectra measured under these conditions exhibit anomalous or normal SEIRAS band shapes. Here, we will perform such a test using CO as test molecule.

Figure 7 shows the SEIRAS spectra obtained with thin gold films of 20 nm made at 1 Å/s, measured in CO-saturated 0.1 M H_2SO_4 solutions, plotted as a function of the applied potential. The reference spectrum was taken at E=0.05 V prior to CO dosing. Clearly, the bands of adsorbed CO gold, at ca 2100 cm^{-1}, are monopolar. With increasing potential, the magnitude of the CO band decreases, due to CO oxidation, in agreement with a previous study by Osawa and coworkers.[78] On the other hand, the presence of CO does not produce any significant effect on the shape or magnitude of the bands due to water and sulfate adsorbed species (see figure 3, measured in the absence of CO, for comparison).

In order to obtain a deeper understanding on the shape of the experimental SEIRAS bands, we performed simulations of the whole SEIRAS spectra using the Fresnel equations for a multilayer system. For the calculations, the optical constants of Si, Au and H_2O have been obtained from the literature.[79,80] For CO, the dielectric function of a damped harmonic oscillator has been used:[65]

$$\varepsilon^2 = n_e^2 + \frac{B}{\nu_0^2 - \nu^2 + i\,\gamma\,\nu}$$

where n_e is the refractive index far away from the resonance (n_e=1), ν is the wavenumber (in cm^{-1}), ν_0 is the wavenumber of the adsorption band maximum (ν_0 =2110 cm^{-1}), i is the imaginary number, γ is the damping constant and determines the width of the adsorption band (γ =20 cm^{-1}), and B represents the amplitude of the resonance and determines the intensity of the band (B =38000 cm^{-2}).

Figure 8 compares the results of the calculations with the experiments. All the experimental data in figure 8 have been obtained with gold thin films of 20 nm deposited at 1 Å/s. Figure 8A shows the calculated spectrum of adsorbed CO as estimated from the ratio in reflectivity of the system Si-Au-CO and Si-Au-air. The experimental CO spectrum corresponds to the reflectivity ratio measured with CO-saturated and Ar-purged 0.1 M H_2SO_4 solutions at E=0.05 V. Figure 8B shows the calculated spectrum of water as obtained from the ration in reflectivity of the system and Si-Au-H_2O and Si-Au-air. Similarly, the experimental spectrum has been obtained from the ratio of the reflectivities of water-covered and dry gold films. Finally, figure 8C plots the calculated and experimental absorption by the thin gold films, where the experimental data has been obtained from transmission spectrum of thin gold films deposited on Si wafers. Overall, the agreement between the calculated and experimental curves is satisfactory, and demonstrates that the SEIRAS spectra reported here are free from optical artifacts.

References:

(1) Zope, B. N.; Hibbitts, D. D.; Neurock, M.; Davis, R. J. *Science* **2010**, *330*, 74-78.

(2) Date, M.; Okumura, M.; Tsubota, S.; Haruta, M. *Angew.Chem.Int.Ed.* **2004**, *43*, 2129-2132.

(3) *Fuel Cell Catalysis: A Surface Science Approach.*; John Wiley and Sons, Inc: Hoboken, New Jersey (USA), 2009.

(4) Stamenkovic, V. R.; Fowler, B.; Mun, B. S.; Wang, G. F.; Ross, P. N.; Lucas, C. A.; Markovic, N. M. *Science* **2007**, *315*, 493-497.

(5) Stamenkovic, V.; Mun, B. S.; Mayrhofer, K. J. J.; Ross, P. N.; Markovic, N. M.; Rossmeisl, J.; Greeley, J.; Norskov, J. K. *Angew.Chem.Int.Ed.* **2006**, *45*, 2897-2901.

(6) Zhang, J.; Sasaki, K.; Sutter, E.; Adzic, R. R. *Science* **2007**, *315*, 220-222.

(7) Strbac, S.; Adzic, R. R. *Electrochim.Acta* **1996**, *41*, 2903-2908.

(8) Strbac, S.; Adzic, R. R. *J.Electroanal.Chem.* **1996**, *403*, 169-181.

(9) Paliteiro, C.; Martins, N. *Electrochim.Acta* **1998**, *44*, 1359-1368.

(10) Hernandez, J.; Solla-Gullon, J.; Herrero, E.; Aldaz, A.; Feliu, J. M. *Journal of Physical Chemistry C* **2007**, *111*, 14078-14083.

(11) Hernandez, J.; Solla-Gullon, J.; Herrero, E. *J.Electroanal.Chem.* **2004**, *574*, 185-196.

(12) El-Deab, M. S.; Ohsaka, T. *Electrochem.Comm.* **2002**, *4*, 288-292.

(13) Henderson, M. A. *Surf.Sci.Rep.* **2002**, *46*, 1-308.

(14) Osawa, M. *Bulletin- Chemical Society of Japan* **1997**, *70*, 2861-2880.

(15) Ataka, K.; Yotsuyanagi, T.; Osawa, M. *J.Phys.Chem.* **1996**, *100*, 10664-10672.

(16) Ataka, K. I.; Osawa, M. *Langmuir* **1998**, *14*, 951-959.

(17) Cai, W.-B.; Wan, L.-J.; Noda, H.; Hibino, Y.; Ataka, K.; Osawa, M. *Langmuir* **1998**, *14*, 6992-6998.

(18) Noda, H.; Ataka, K.; Li-Jun-Wa; Osawa, M. *Surf.Sci.* **1999**, *427-428; 1 June 1999*, 190-194.

(19) Noda, H.; Minoha, T.; Wan, L. J.; Osawa, M. *J.Electroanal.Chem.* **2000**, *481*, 62-68.

(20) Cai, W.-B.; Amano, T.; Osawa, M. *J.Electroanal.Chem.* **2001**, *500*, 147-155.

(21) Noda, H.; Wan, L. J.; Osawa, M. *Phys.Chem.Chem.Phys.* **2001**, *3*, 3336-3342.

(22) Wandlowski, Th.; Ataka, K.; Mayer, D. *Langmuir* **2002**, *18*, 4331-4341.

(23) Pronkin, S.; Wandlowski, Th. *J.Electroanal.Chem.* **2003**, *550-551*, 131-147.

(24) Wandlowski, T.; Ataka, K.; Pronkin, S.; Diesing, D. *Electrochim.Acta* **2004**, *49*, 1233-1247.

(25) Pronkin, S.; Wandlowski, T. *Surf.Sci.* **2004**, *573*, 109-127.

(26) Han, B.; Li, Z.; Pronkin, S.; Wandlowski, Th. *Canadian Journal of Chemistry* **2004**, *82*, 1481-1494.

(27) Pronkin, S.; Hara, M.; Wandlowski, T. *Russ.J.Electrochem.* **2006**, *42*, 1177-1192.

(28) Futamata, M. *Surf.Sci.* **1999**, *427-428*, 179-183.

(29) Futamata, M. *Chem.Phys.Lett.* **2000**, *317*, 304-309.

(30) Futamata, M. *J.Phys.Chem.B* **2001**, *105*, 6933-6942.

(31) Futamata, M. *J.Electroanal.Chem.* **2003**, *550-551*, 93-103.

(32) Berna, A.; Delgado, J. M.; Orts, J. M.; Rodes, A.; Feliu, J. M. *Langmuir* **2006**, *22*, 7192-7202.

(33) Delgado, J. M.; Berna, A.; Orts, J. M.; Rodes, A.; Feliu, J. M. *Journal of Physical Chemistry C* **2007**, *111*, 9943-9952.

(34) Berna, A.; Delgado, J. M.; Orts, J. M.; Rodes, A.; Feliu, J. M. *Electrochim.Acta* **2008**, *53*, 2309-2321.

(35) Delgado, J. M.; Blanco, R.; Orts, J. M.; Perez, J. M.; Rodes, A. *Journal of Physical Chemistry C* **2009**, *113*, 989-1000.

(36) The magnitude of the voltammetric current was slightly smaller with gold thin films deposited at 0.1 Å/s, which is probably due to a smaller roughness factor.

(37) Magnussen, O. M.; Hageböck, J.; Hotlos, J.; Behm, R. J. *Faraday Discuss.* **1992**, *94*, 329-338.

(38) Hamelin, A. *J.Electroanal.Chem.* **1996**, *407*, 1-11.

(39) Chen, N.; Blowers, P.; Masel, R. I. *Surf.Sci.* **1999**, *419*, 150-157.

(40) Simeone, F. C.; Kolb, D. M.; Venkatachalam, S.; Jacob, T. *Surf.Sci.* **2008**, *602*, 1401-1407.

(41) Meng, S.; Wang E.G.; Gao, S. *Phys.Rev.B* **2004**, *69*, 195404.

(42) Santana, J. A.; Cabrera, C. R.; Ishikawa, Y. *Phys.Chem.Chem.Phys.* **2010**, *12*, 9526-9534.

(43) Simeone, F. C.; Kolb, D. M.; Venkatachalam, S.; Jacob, T. *Angew.Chem.Int.Ed.* **2007**, *46*, 8903-8906.

(44) Polop, C.; Rosiepen, C.; Bleikamp, S.; Drese, R.; Mayer, J.; Dimyati, A.; Michely, Th. *New Journal of Physics* **2007**, *9*, 74.

(45) Rost, M. J. *Physical Review Letters* **2007**, *99*, 266101.

(46) Delgado, J. M.; Orts, J. M.; Perez, J. M.; Rodes, A. *J.Electroanal.Chem.* **2008**, *617*, 130-140.

(47) Sato, K.; Yoshimoto, S.; Inukai, J.; Itaya, K. *Electrochem.Comm.* **2006**, *8*, 725-730.

(48) Dretschkow, T.; Wandlowski, T. *Ber.Bunsen-Ges.* **1997**, *101*, 749-757.

(49) Tielrooij, K. J.; Garcia-Araez, N.; Bonn, M.; Bakker, H. J. *Science* **2011**, *328*, 1006-1009.

(50) Osawa, M.; Ataka, K. I.; Yoshii, K.; Nishikawa, Y. *Appl.Spectrosc* **1993**, *47*, 1497-1502.

(51) Stretch and bending modes in the plane perpendicular to the surface will be inactive, while the bending mode in the plane parallel to the surface will be hindered by the interaction with the gold surface.

(52) Michaelides, A.; Ranea, V. A.; de Andres, P. L.; King, D. A. *Phys.Rev.Lett.* **2003**, *90*, 216102.

(53) Osawa, M.; Tsushima, M.; Mogami, H.; Samjeské, G.; Yamakata, A. *Journal of Physical Chemistry C* **2008**, *112*, 4248-4256.

(54) Edens, G. J.; Gao, X.; Weaver, M. J. *J.Electroanal.Chem.* **1994**, *375*, 357-366.

(55) Wan, L. J.; Yau, S. L.; Itaya, K. *J.Phys.Chem.* **1995**, *99*, 9507-9513.

(56) Funtikov, A. M.; Stimming, U.; Vogel, R. *J.Electroanal.Chem.* **1997**, *428*, 147-153.

(57) Wan, L.-J.; Hara, M.; Inukai, J.; Itaya, K. *J.Phys.Chem.B* **1999**, *103*, 6978-6983.

(58) Wan, L. J.; Suzuki, T.; Sashikata, K.; Okada, J.; Inukai, J.; Itaya, K. *J.Electroanal.Chem.* **2000**, *484*, 189-193.

(59) Kim, Y. G.; Soriaga, J. B.; Vigh, G.; Soriaga, M. P. *J.Colloid Interface Sci.* **2000**, *227*, 505-509.

(60) Shi, Z.; Lipkowski, J.; Gamboa, M.; Zelenay, P.; Wieckowski, A. *J.Electroanal.Chem.* **1994**, *366*, 317-326.

(61) Nishikawa, Y.; Fujiwara, K.; Ataka, K.; Osawa, M. *Anal.Chem.* **1993**, *65*, 556-562.

(62) Bjerke, A. E.; Griffiths, P. R.; Theiss, W. *Anal.Chem.* **1999**, *71*, 1967-1974.

(63) Lu, G. Q.; Sun, S. G.; Cai, L. R.; Chen, S. P.; Tian, Z. W. *Langmuir* **2000**, *16*, 778-786.

(64) Krauth, O.; Fahsold, G.; Magg, N.; Pucci, A. *J.Chem.Phys.* **2000**, *113*, 6330-6333.

(65) Bürgi, T. *Phys.Chem.Chem.Phys.* **2001**, *3*, 2124-2130.

(66) Ferri, D.; Bürgi, T.; Baiker, A. *J.Phys.Chem.B* **2001**, *105*, 3187-3195.

(67) Park, S.; Tong, Y.; Wieckowski, A.; Weaver, M. J. *Electrochem.Comm.* **2001**, *3*, 509-513.

(68) Lin, W. G.; Sun, S. G.; Zhou, Z. Y.; Chen, S. P.; Wang, H. C. *J.Phys.Chem.B* **2002**, *106*, 11778-11783.

(69) Miki, A.; Ye, S.; Osawa, M. *Chem.Commun.* **2002**, 1500-1501.

(70) Chen, Y. J.; Sun, S. G.; Chen, S. P.; Li, J. T.; Gong, H. *Langmuir* **2004**, *20*, 9920-9925.

(71) Suzuki, Y.; Goto, S.; Umetsu, H. *Eur.Phys.J.D* **2005**, *33*, 201-205.

(72) Heaps, D. A.; Griffiths, P. R. *Vibrational Spectroscopy* **2006**, *42*, 45-50.

(73) Erbe, A.; Bushby, R. J.; Evans, S. D.; Jeuken, L. J. C. *J.Phys.Chem.B* **2007**, *111*, 3515-3524.

(74) Bukasov, R.; Shumaker-Parry, J. S. *Anal.Chem.* **2009**, *81*, 4531-4535.

(75) Fano, U. *Phys.Rev.* **1961**, *124*, 1866-1878.

(76) Langreth, D. C. *Physical Review Letters* **1985**, *54*, 126-129.

(77) Persson, B. N. J.; Volokitin, A. I. *Surf.Sci.* **1994**, *310*, 314-336.

(78) Sun, S.-G.; Cai, W.-B.; Wan, L.-J.; Osawa, M. *J.Phys.Chem.B* **1999**, *103*, 2460-2466.

(79) Handbook of optical constants of solids *Handbook of optical constants of solids*; Academic Press: London, 1985; p Academic Press Handbook Series.

(80) Bertie, J. E.; Ahmed, M. K.; Eysel, H. H. *J.Phys.Chem.* **1989**, *93*, 2210-2218.

Figures

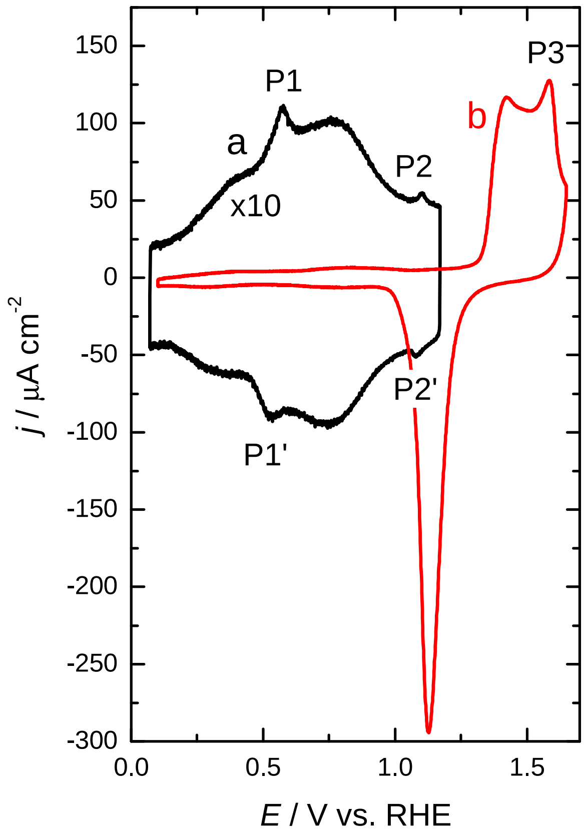

Figure 1. Steady-state cyclic voltammograms of a thin gold film of 20 nm, deposited at 1 Å/s, and put in contact with 0.1 M H_2SO_4. Scan rate=50 mV/s. Curve a has been expanded 10 times.

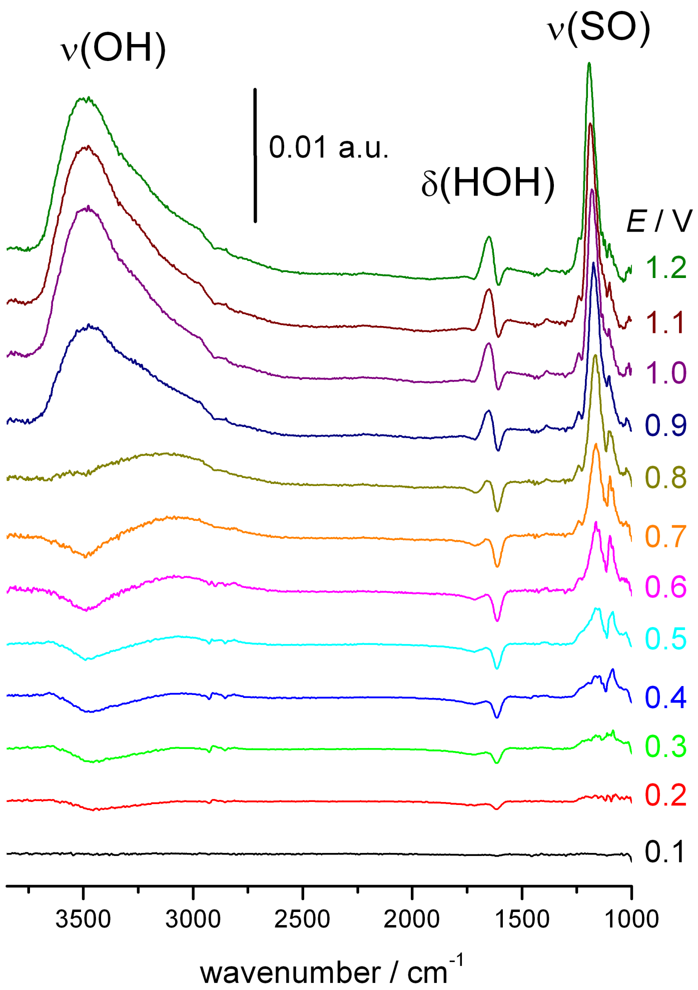

Figure 2. SEIRAS spectra at different potentials in 0.1 M H_2SO_4, measured with a gold thin film of 20 nm deposited at 0.1 Å/s. The reference spectrum was taken at E_{ref}=0.05V.

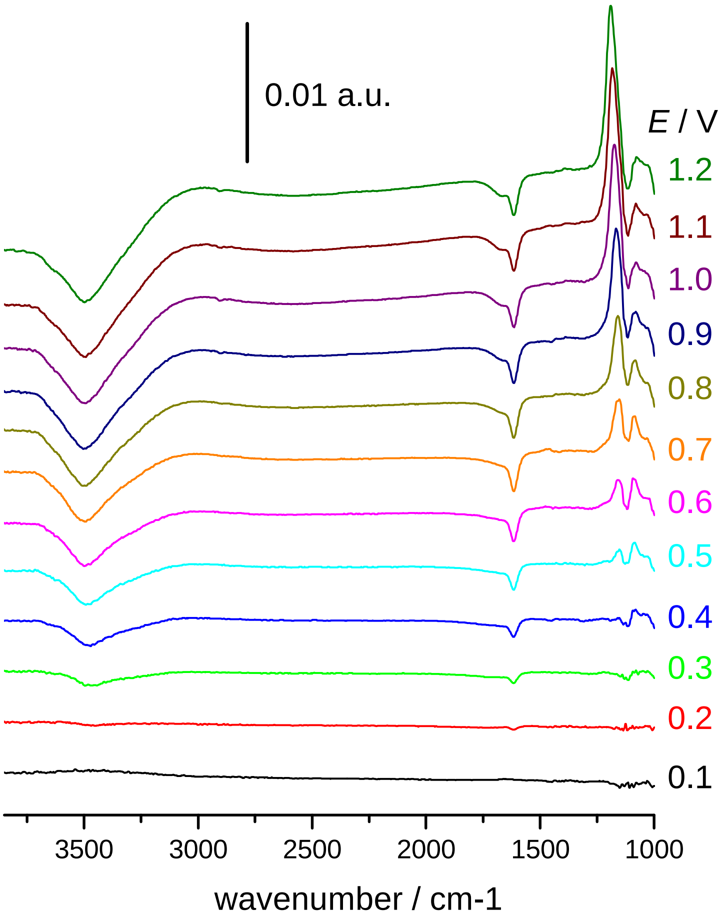

Figure 3. As in figure 2, but with the gold thin film deposited at 1 Å/s.

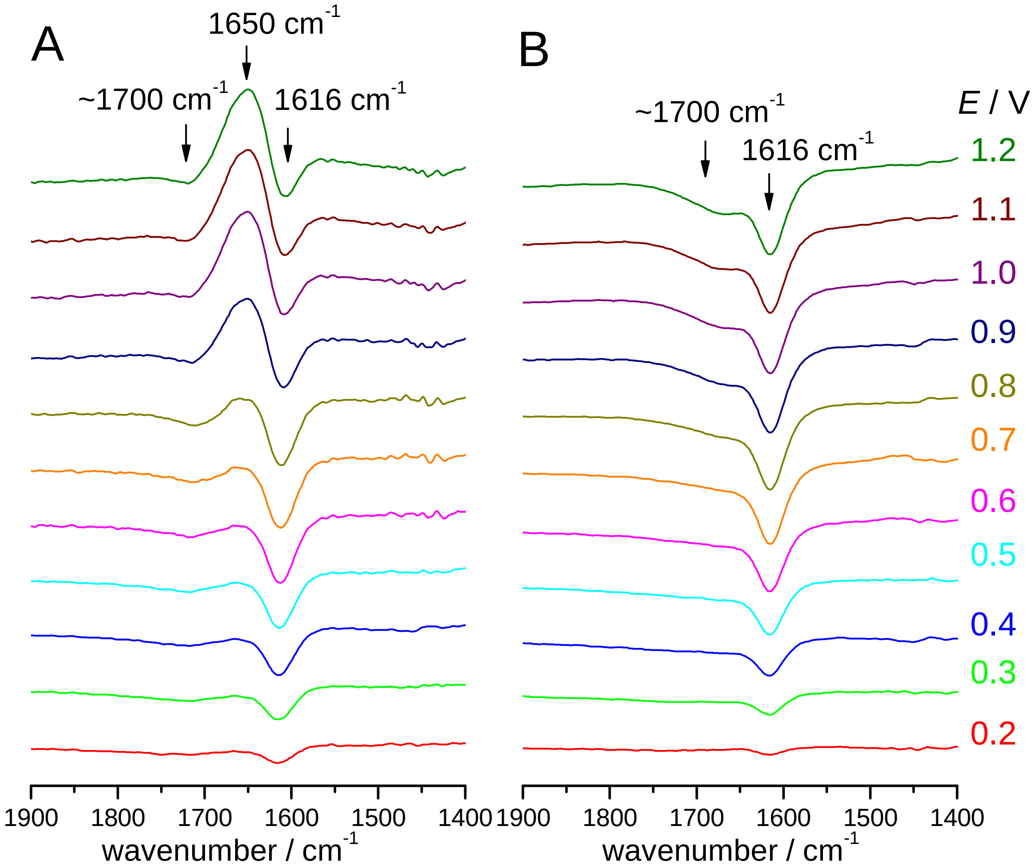

Figure 4. Enlargement within the bending mode region of the spectra shown in: A) figure 2, and B) figure 3.

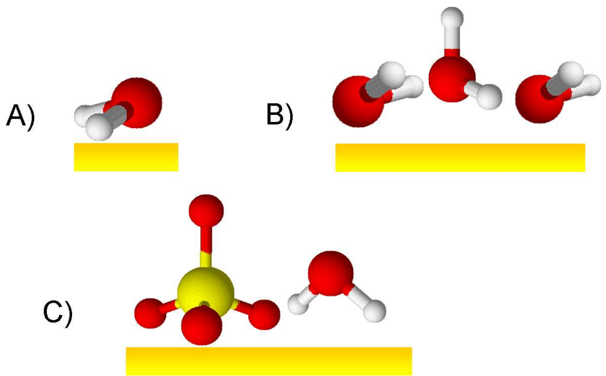

Figure 5. Proposed model structures of water adsorbed on gold electrodes.

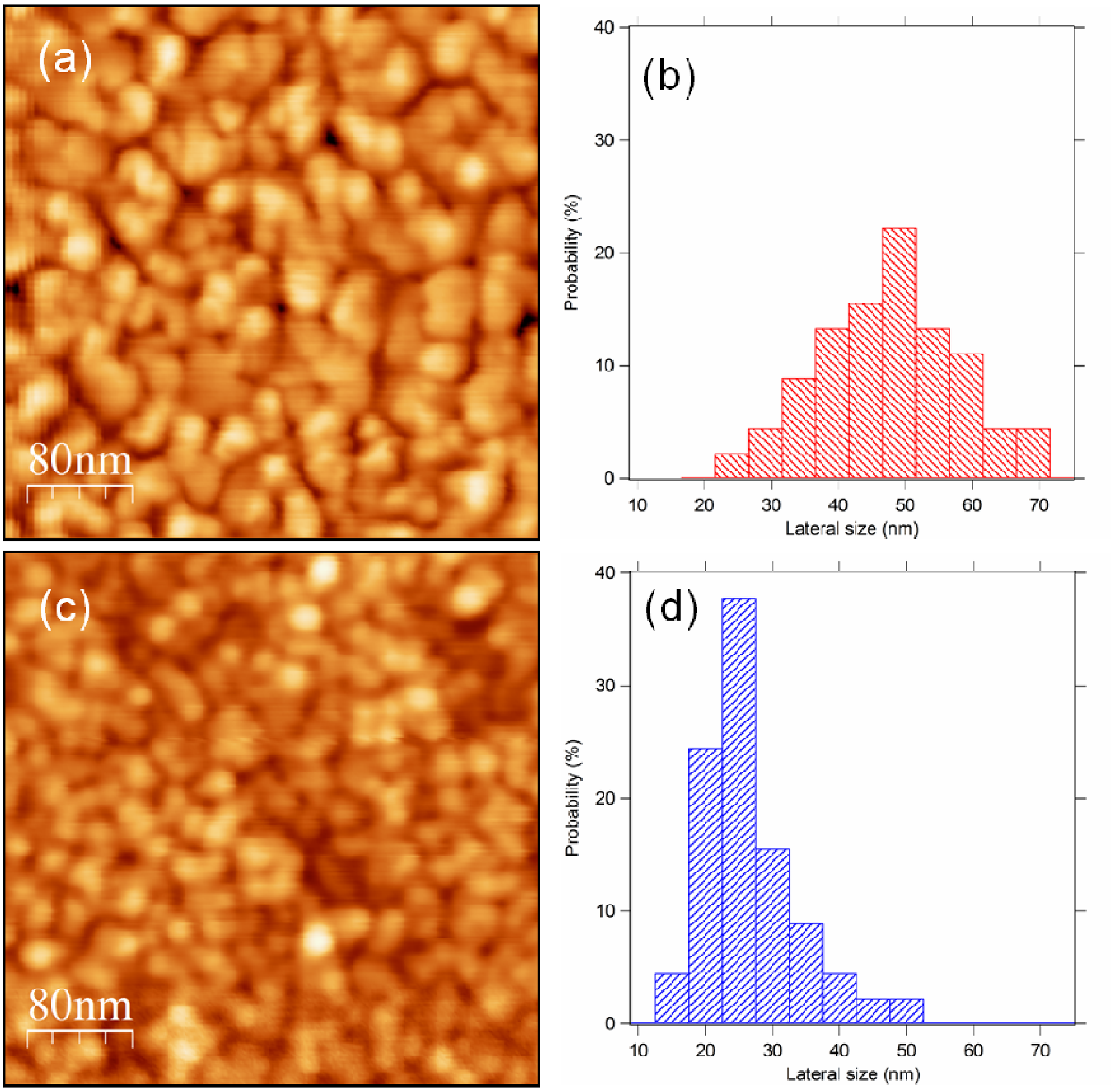

Figure 6. AFM images (a, c) and histograms of the particle size distribution (b, d). Images (a) and (b) correspond to the sample grown at 0.1 Å/s, and images (c) and (d) to the sample grown at 1 Å/s. The lateral size of the grains is 47±11 nm (a,b) and 27±8 nm (c,d). The total vertical scale is 11 nm (a) and 7 nm (c).

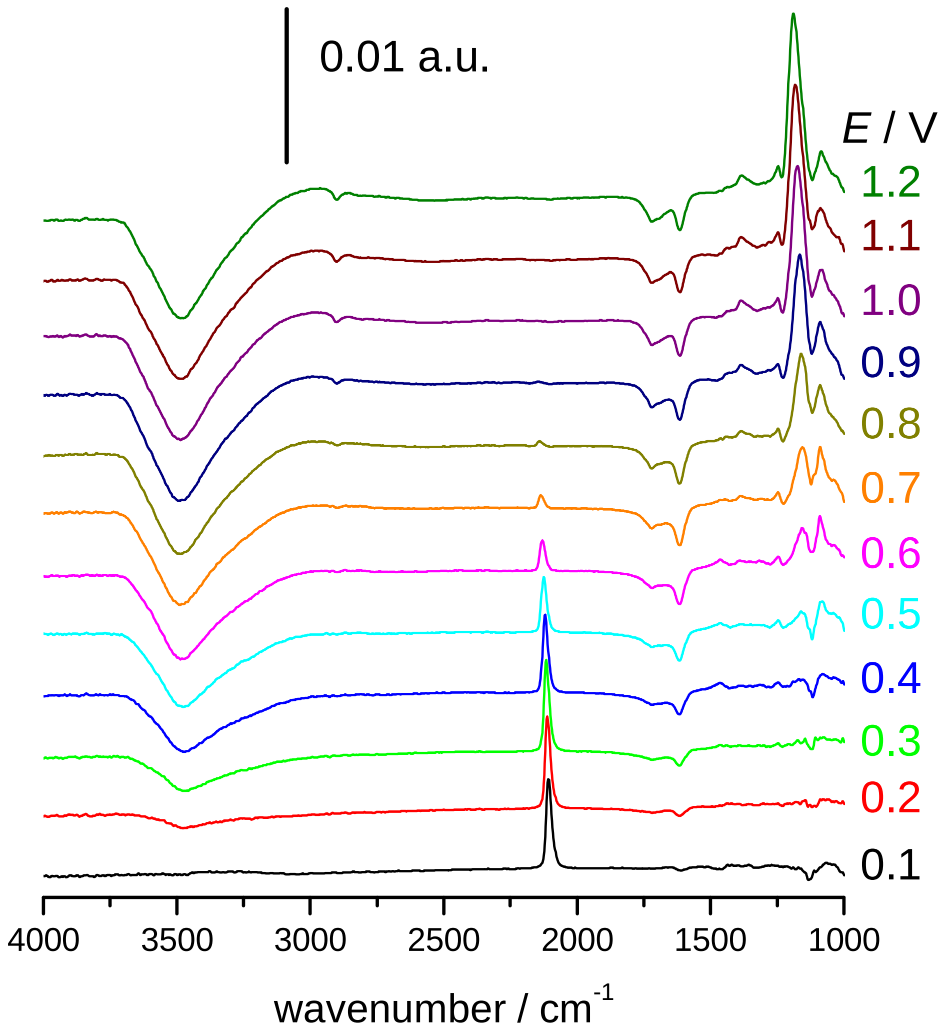

Figure 7. As in figure 3 but in CO-saturated solutions.

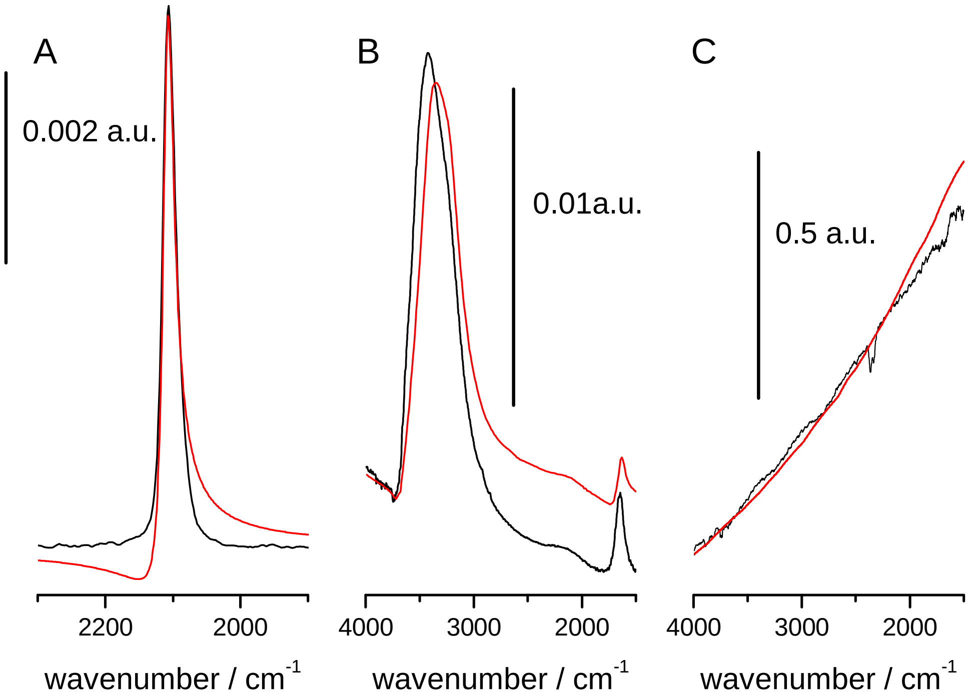

Figure 8. Experimental (black curves) and calculated (red curves) absorption spectra of CO (A), water (B) and gold thin films (C). See text for details.

TOC graphic

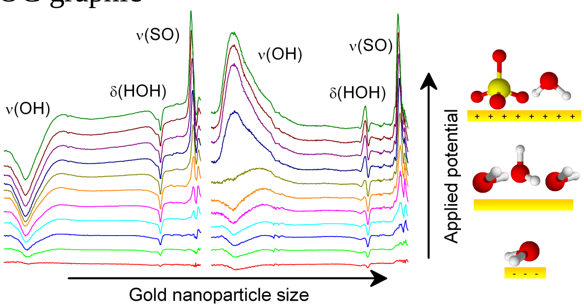

ν(SO)
ν(OH)
δ(HOH)
ν(OH)
ν(SO)
δ(HOH)
Applied potential
Gold nanoparticle size